Electronic Supplementary Information

Dual Catalytic Activity of Cucurbit[7]uril-functionalized Metal Alloy Nanocomposite for Sustained Hydrogen Generation: Hydrolysis of Ammonia Borane and Electrocatalyst for Hydrogen Evolution Reaction

Dwaipayan Majumder,[a,b] Suprotim Koley,[a] Atanu Barik,[a,b] Priyanka Ruz,[c] Seemita Banerjee,[b,c] Bathula Viswanadh,[d] Nilotpal Barooah,[a,b] Vaidehi S. Tripathi,[a] Vasanthakumaran Sudarsan,[b,c] Awadhesh Kumar,[a,b] Avesh Kumar Tyagi,[b,c] Achikanath C. Bhasikuttan*[ab] and Jyotirmayee Mohanty*[ab]

[a]Radiation & Photochemistry Division, Bhabha Atomic Research Centre, Mumbai 400085, India . [b]Homi Bhabha National Institute, Training School Complex, Anushaktinagar, Mumbai 400094, India . [c]Chemistry Division, Bhabha Atomic Research Centre, Mumbai 400085, India , [d]Materials Science Division, Bhabha Atomic Research Centre, Mumbai 400085, India.

Synthesis of Co:Ni:CB7 nanocomposites

The metal alloy nanoparticles were synthesised by chemical reduction method using sodium borohydrate ($NaBH_4$) at room temperature. Briefly, 15 mM of metal salts (mixture of cobalt acetate and nickel chloride) and 0.5 mM of host CB7 were dissolved in 25 ml of nonpure water. To the Co:Ni mixture solution 150 mM of 25 ml $NaBH_4$ solution was added slowly under constant stirring. Within few minutes of the addition of $NaBH_4$, black colour suspension of fine particles appeared. The black suspension was centrifuged under 10000 RPM for 10 minutes and black solid nano composites were obtained. These nanocomposites were washed with water under centrifugation once to remove excess $NaBH_4$. Finally, these nanoparticles were washed with methanol and dried under IR lamp. Different compositions of Co and Ni in the nanocomposites were achieved by taking different stoichiometric ratio of Co and Ni salts by maintaining a total metal concentration of 15 mM. The Co:Ni nanoalloys with different compositions were also prepared using above method without adding CB7.

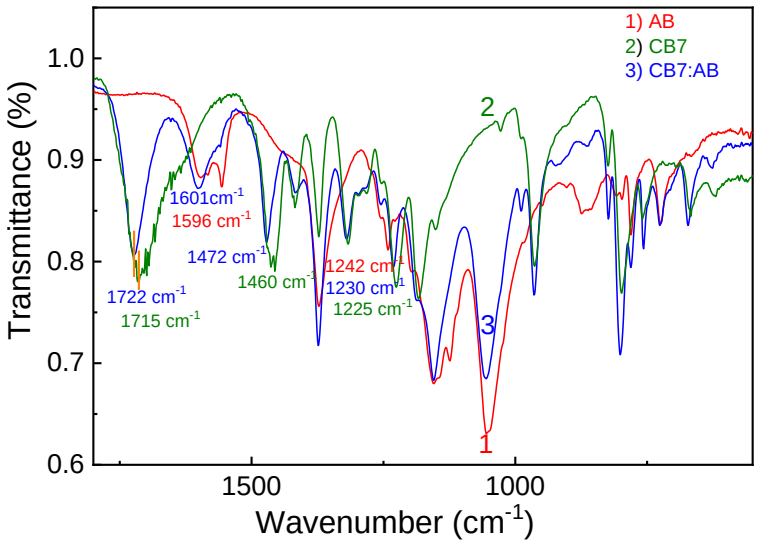

Fig. S1 FTIR of AB, CB7 and CB7:AB systems.

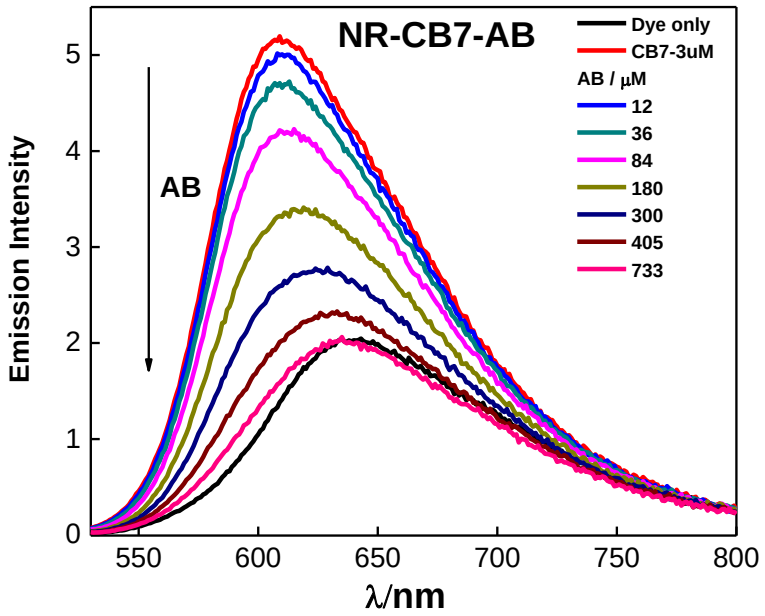

Fig. S2 Fluorescence spectrum of cucurbit[7]uril-complexed neutral red (NR) in the presence of AB.

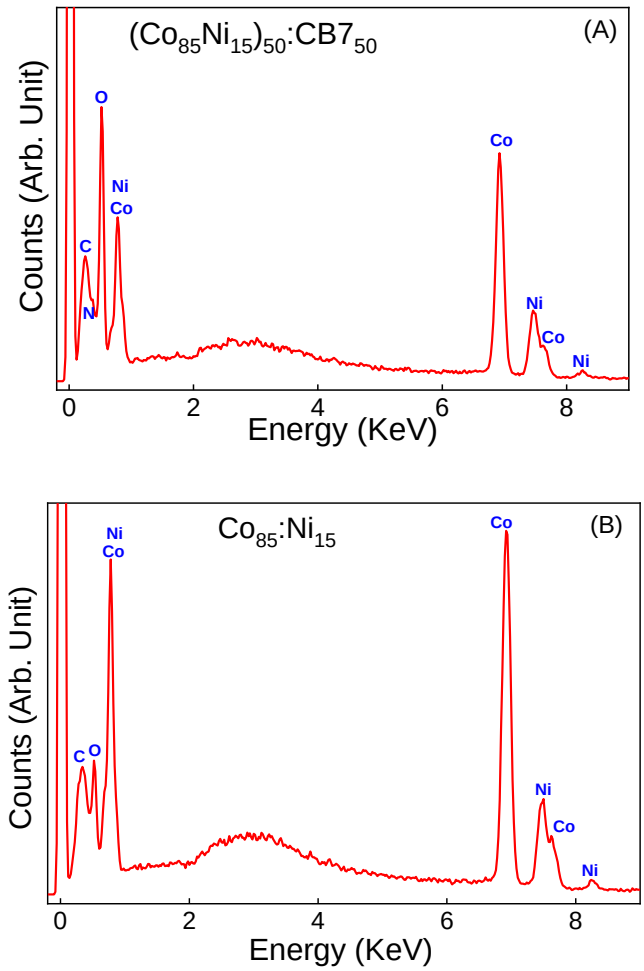

Fig. S3 EDS spectra (A and B) of $(Co_{85}:Ni_{15})_{50}:(CB7)_{50}$ and $(Co_{85}:Ni_{15})$ nanoalloy composites, respectively.

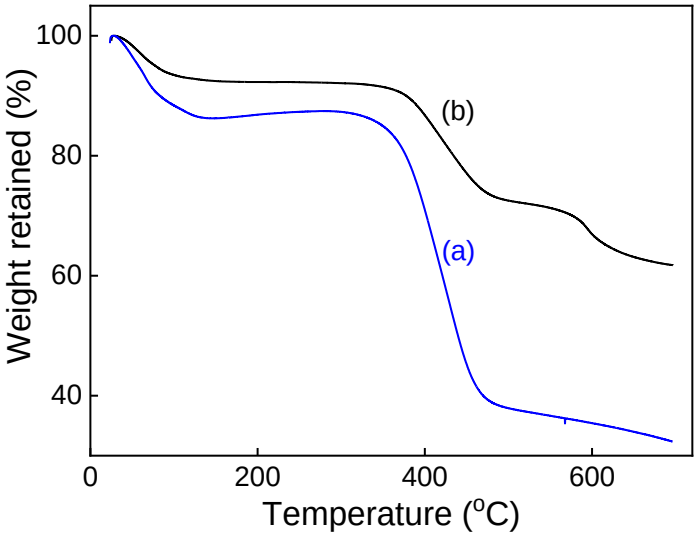

Fig. S4 Thermogravimetric traces of CB7 (a) and $(Co_{85}:Ni_{15})_{50}:(CB7)_{50}$ (b).

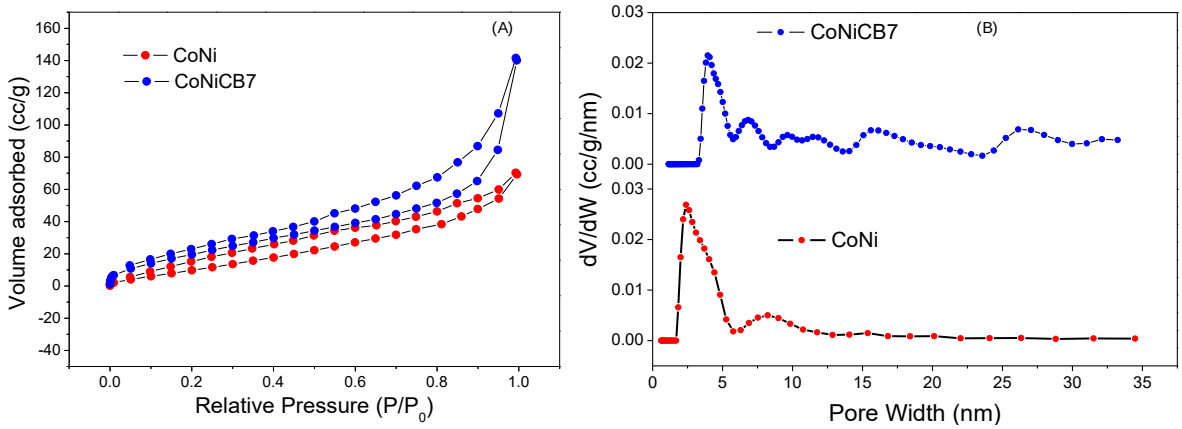

Fig. S5 (A) N_2 adsorption-desorption isotherm at 77 K for Co_{85}:Ni_{15} and $(Co_{85}$:$Ni_{15})_{50}$:$(CB7)_{50}$. (B) Corresponding pore size distributions. Co_{85}:Ni_{15} shows 2 prominent peaks at around 2.35 nm and 8.3 nm. $(Co_{85}$:$Ni_{15})_{50}$:$(CB7)_{50}$ shows hierarchical porosity with peak maxima around 3.9, 6.9, 9.6, 11.7, 15.9 and 26.4 nm.

Table S1. Textual properties of Co_{85}:Ni_{15} and $(Co_{85}$:$Ni_{15})_{50}$:$(CB7)_{50}$ nanocomposites derived from N_2 adsorption-desorption isotherm.

Sample	**Textural Properties**	
	V_p[a] (cc/g)	**D_{pore}[b] (nm)**
Co_{85}:Ni_{15}	0.107	2.38
$(Co_{85}$:$Ni_{15})_{50}$:$(CB7)_{50}$	0.217	3.94

[a] Total pore volume, [b] Average pore width

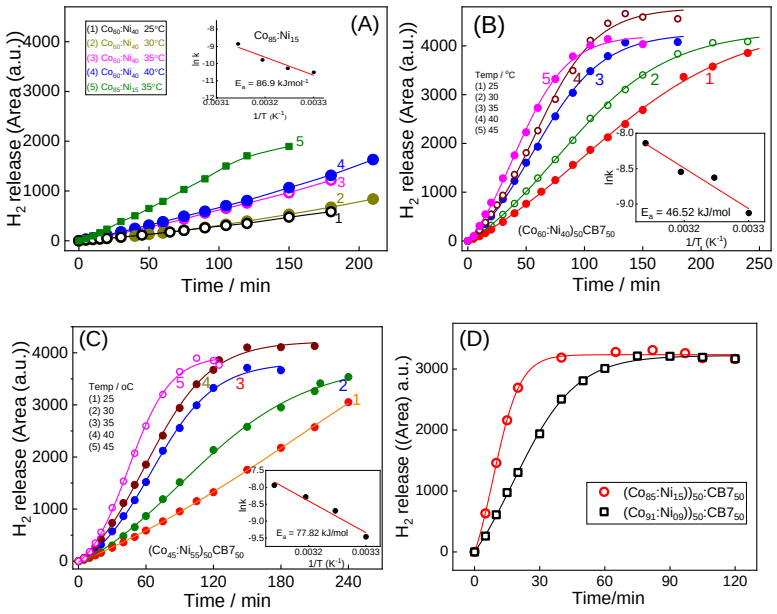

Fig. S6 H_2 release yield measurements carried out with different compositions of the nanoalloys (Co_{60}:Ni_{40}; Co_{85}:Ni_{15}) at different temperatures (**A**); H_2 release from the hydrolysis of AB with $(Co_{60}:Ni_{40})_{50}$:$(CB7)_{50}$ (**B**); $(Co_{45}:Ni_{55})_{50}$:$(CB7)_{50}$ (**C**) and at different temperatures. (**D**) represent the comparison of the $(Co_{91}:Ni_{09})_{50}$:$(CB7)_{50}$ with $(Co_{85}:Ni_{15})_{50}$:$(CB7)_{50}$ at 35°C showing decrease in the H_2 release rate with higher Co content. Inset of A, B and C shows the Arrhenius plot (ln k vs 1/T) for the AB system in the presence of Co_{85}:Ni_{15}, $(Co_{60}:Ni_{40})_{50}$:$(CB7)_{50}$ and $(Co_{45}:Ni_{55})_{50}$:$(CB7)_{50}$, respectively.

Synthetic Procedure for AB regeneration

Step-I (Conversion of NH_4BO_2 to boric acid)

Acidification of NH_4BO_2 solution with sulfuric acid led to the formation of boric acid which crystallized at very low temperature (~5°C). The FT-IR signals of synthesized boric acid matches well with those of commercial boric acid obtained from Sigma-Aldrich.

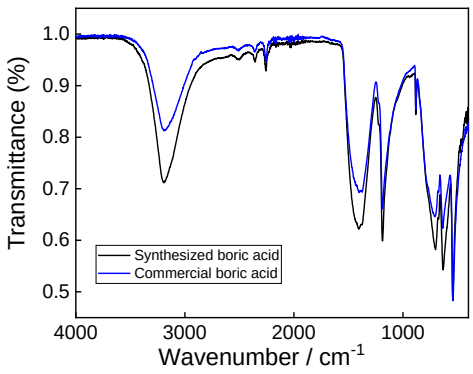

Fig. S7 FT-IR spectra of both synthesized and commercial boric acid.

Step-II (Conversion of boric acid to trimethyl borate)

Esterification of boric acid was carried out in methanol in presence of low concentration of sulfuric acid as catalyst to synthesize trimethyl borate ($B(OMe)_3$). Due to the very small difference in the boiling point of both methanol and $B(OMe)_3$, azeotropic mixture of methanol and $B(OMe)_3$ was obtained and fractional distillation was carried out to get the pure $B(OMe)_3$. The synthesized $B(OMe)_3$ was characterized by FT-IR and GC-MS. The FT-IR signal at 1353 cm^{-1} due to $-CH_3$ bending in $B(OMe)_3$ and GC-MS signals at 104 due to the molecular peak and other fragmented signals matches well with the signals of trimethyl borate from GC-MS library.

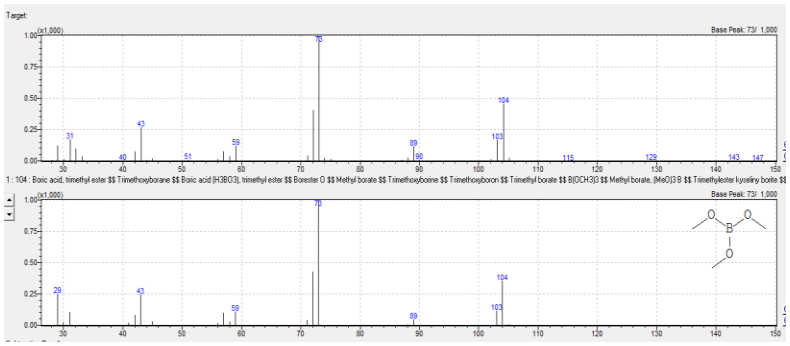

Fig. S8 GC-MS spectra of both synthesized and standard trimethyl borate.

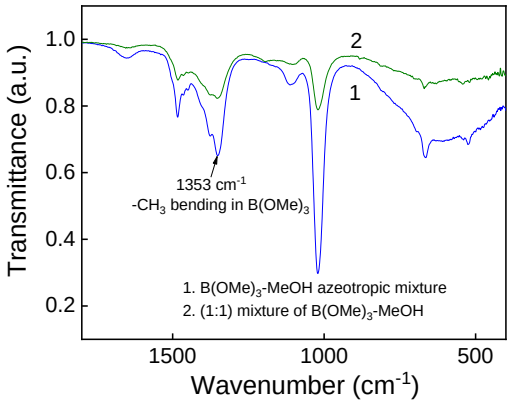

Fig. S9 FT-IR spectra of both synthesized and commercial trimethyl borate.

Step-III (Conversion of trimethyl borate to ammonia borane)

Trimethyl borate was reduced with lithium aluminium hydride in the presence of NH_4Cl in THF to synthesize ammonia borane. The FT-IR and ^1H NMR spectra of regenerated ammonia borane matches well with that of commercially available ammonia borane.

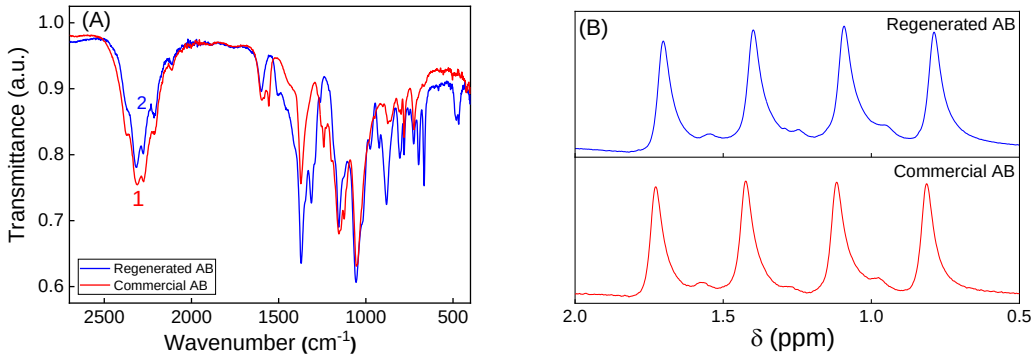

Fig. S10 FT-IR (**A**) and ^1H NMR (**B**) spectra of both regenerated and commercially available ammonia borane.

Chronopotentiometry of Co:Ni and Co:Ni:CB7

Beside catalytic efficiency, stability of catalyst was also tested by 8 hours of chronopotentiometry. It took some times for Co:Ni to achieve the current density of -10 mA/cm^2 whereas Co:Ni:CB7 showed stable current density from the starting point. Co:Ni nanoparticles first achieved -10 mA/cm^2 current below -0.5 V (i.e. -0.488 V) vs RHE within 30 minutes (**Fig. S11 A**). Later it's activity reduced and after almost 2 hours it achieved stable current density at above -0.5 V. Whereas Co:Ni:CB7 maintained a constant potential throughout the whole time (**Fig. S11 B**).

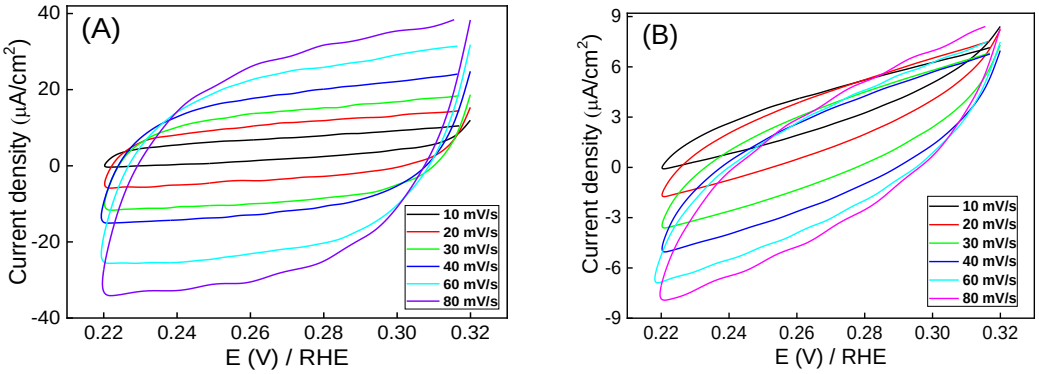

Fig. S11 Cyclic voltammograms for the $(Co_{85}:Ni_{15})_{50}:(CB7)_{50}$ (**A**) and $Co_{85}:Ni_{15}$ (**B**) nanocomposites at different scan rates.

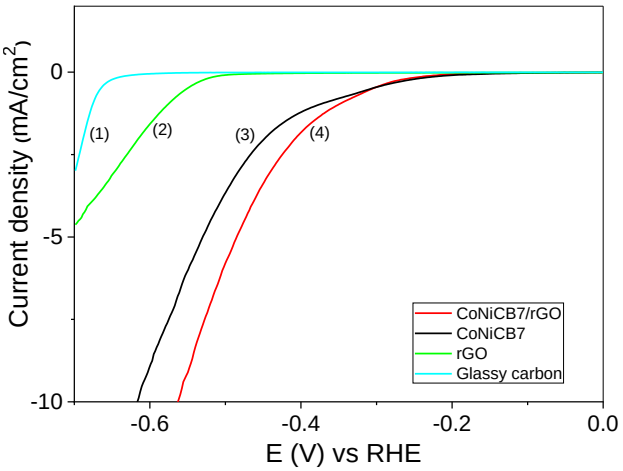

Fig. S12 Linear sweep voltammograms (LSV) of the GC electrode coated with: no coating (1), rGO (2), Co:Ni:CB7 (3) and Co:Ni:CB7-rGO (4).